Pergamon

Geochimica et Cosmochimica Acta, Vol. 67, No. 16, pp. 3005–3014, 2003

0016-7037/03 $30.00 + .00

doi:10.1016/S0016-7037(00)00303-X

# Hydrosulfide/sulfide complexes of copper(I): Experimental confirmation of the stoichiometry and stability of $Cu(HS)_2^-$ to elevated temperatures

B. W. MOUNTAIN[1,*] and T. M. SEWARD[2]

[1]Institute of Geological and Nuclear Sciences, Wairakei Research Centre, Private Bag 2000, Taupo, New Zealand
[2]Institute for Mineralogy and Petrology, Eidgenössiche Technische Hochschule (ETH), 8092 Zürich, Switzerland

(*Received October* 16, 2002; revised 3 April 2003; *accepted in revised form April* 3, 2003)

**Abstract**—The solubility of chalcocite has been measured over the temperature range 35–95°C at pH 6.5–7.5 in aqueous hydrosulfide solutions in order to determine the stability constants of the $Cu(HS)_2^-$ complex. A heated flow-through system was used in which solutions are collected at temperature to avoid the problem of copper precipitation due to quenching. The quality of the data was sufficient to resolve a 0.1 log unit increase of the dissolution/complexation equilibrium constant with each 10°C increase in temperature. The equilibrium constants were fit using previously published methods to obtain the values of thermodynamic parameters for the $Cu(HS)_2^-$ complexation reaction. To compare results with predictive techniques, one-term and two-term isocoulombic extrapolation methods were applied to the stability constants measured below 100°C. The two-term extrapolation to 350°C showed excellent agreement with the derived constants proving its applicability to soft metal–soft ligand interactions. The one-term method gave a reasonable agreement but deviated about one logarithmic unit at 350°C. This is attributed to differences in energetic, volumetric, and structural properties of the reactants and products. Speciation calculations show that at low temperatures (<150°C), the hydrosulfide complexes of copper will dominate over chloride complexes at low salinites (<0.1 mol $kg^{-1}$) while at higher temperatures, chloride complexes will be dominant under most geological conditions. Only in solutions with high reduced sulfur content and alkaline pH values will hydrosulfide complexes predominate and may play a role in the generation of economic copper mineralization. 

## 1. INTRODUCTION

The use of numerical modeling to simulate geochemical processes occurring in the natural environment has become a standard technique. Programs such as Geochemist's Workbench (Bethke, 1996), CHILLER/SOLVEQ (Reed, 1982), and SUPCRT92 (Johnson et al., 1992) are frequently encountered when reading published works on geofluid speciation and fluid-rock interaction. The databases supplied with these programs contain numerous aqueous species whose thermodynamic parameters are derived either by fitting empirical data or by predictive methods. Many important metal-ligand interactions, however, still suffer from a lack of ambient temperature thermodynamic data and stoichiometries. As a result, they cannot be included in geochemical modeling program databases. This absence of data becomes acute at high temperature where most metal-ligand-mineral systems are at best poorly understood. The acquisition of thermodynamic data thus remains essential to the study of the behavior of metals and nonmetals in the natural environment. It is unlikely that we will be able to experimentally determine the stabilities and stoichiometries of all metal-ligand interactions at all temperatures and pressures but as more are acquired, thermodynamic databases will become more comprehensive and predictive methods can be improved.

This study focuses on the complexation of copper in solutions containing the hydrosulfide ligand, species that are not currently contained in the databases of the most-frequently encountered modeling programs. Mountain and Seward (1999) determined the stoichiometry and stability of the copper hydrosulfide complexes and found these to include the $Cu(HS)_2^-$ complex at near neutral pH values and the $Cu_2S(HS)_2^{2-}$ complex at basic pH. They also proposed the existence of the $CuHS^o$ complex at low pH and estimated its stability based on the speciation schemes of other $d^{10}$ metal-sulfide complexes and linear free energy relationships. The high temperature experimental data of Crerar and Barnes (1976) were refitted assuming that $CuHS^o$ and $Cu(HS)_2^-$ were the complexes present in their experiments. This speciation model gave a reasonable agreement with the measured solubilities between 200 and 350°C allowing the estimation of stability constants for these species in this temperature range. The lower temperature data of Crerar and Barnes (1976) could not be included in this reinterpretation because of a lack of sufficient data points. A high degree of extrapolation to 350°C was necessary and therefore the derived stability constants above 25°C were approximations.

The goals of this study were to measure the stability constant of the $Cu(HS)_2^-$ complex up to 100°C at several temperatures and to predict, using these measurements, the value of this constant at higher temperatures. If a favorable comparison between the predictions and the stability constants estimated using the experimental data of Crerar and Barnes (1976) were found, this would support the hypothesis that this complex is important at temperatures up to 350°C. It would also provide a high degree of confidence in the thermodynamic data derived from the entire data set. The $CuHS^o$ and $Cu_2S(HS)_2^{2-}$ complexes could not be included in this study because of extremely low $Cu_2S$ solubilities at low pH and temperature and the lack of experimental data at high pH and temperature. Mountain and Seward (1999) have shown that $CuHS^o$ may be the major

* Author to whom correspondence should be addressed (b.mountain@gns.cri.nz).

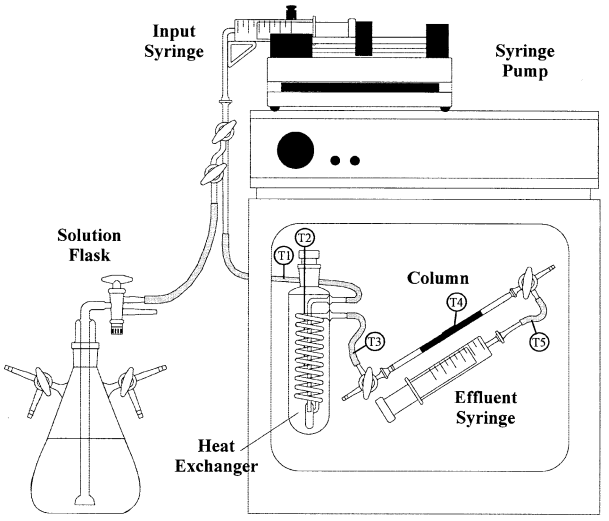


Fig. 1. Heated flow through apparatus used to measure chalcocite solubility to 95°C. Aqueous sulfide solutions are prepared in the solution flask, forced into the input syringe, and pumped into the oven where they pass through the water-filled heat exchanger and the chalcocite-packed column. The effluent is collected in the effluent syringe at oven temperature thereby avoiding quenching. T1–T5 show positions of thermocouples used to monitor temperature along the flow path. The experimental temperature is taken as the average between T3 and T5.

hydrosulfide complex of copper in most hydrothermal solutions at acidic pH values, however, the chloride complexes of copper are expected to be dominant under these conditions. The $Cu_2S(HS)_2^{2-}$ complex is unlikely to be important in most geologic situations as it would require highly basic pH values at higher temperatures.

## 2. EXPERIMENTAL METHODS

The experimental methods used in this study are similar to those described in Mountain and Seward (1999) and full details may be found in that contribution. Chalcocite was synthesized hydrothermally in sealed glass ampoules using copper powder, sulfur pieces and $NH_4Cl$ solution. The glass ampoules were sealed in stainless steel autoclaves into which an appropriate amount of water was added to maintain a confining pressure. The autoclaves were placed in an oven kept at 300°C for one to two weeks. X-ray diffraction analysis confirmed that only well-crystallized chalcocite was present.

A continuous flow-through method was used as an alternative method to measure the solubility of chalcocite in hydrosulfide solutions (Fig. 1). This method overcomes some of the difficulties encountered in batch type experiments such as high fluid to mineral surface area ratios, few replicate analyses, small sample size, and long experimental times resulting in the loss or oxidation of volatile species (e.g., $H_2S$). The flow-through column is constructed entirely of glass components, consisting of the input syringe, injection stem, water-filled heat exchanger, chalcocite-packed column, exit stem and effluent syringe. Plastic PVC tubing connects the components. Temperature is maintained by placing the heat exchanger, column, exit stem and effluent syringe in a heated oven. This allows the sample to accumulate in the effluent syringe at the experimental temperature and thus quenching problems are avoided. Five K-type thermocouples were placed in the flow-through path to monitor experimental temperatures and ensure that the solution had reached the desired temperature once it entered the column. The column temperature was taken as the average of the readings from the thermocouples inserted through the PVC tubing at the beginning and end of the column. No noticeable deterioration of the thermocouples was noted due to contact with the experimental solutions. A syringe pump maintained solution flow with a variable flow rate between 0.1 to 1000 ml/h. Several initial experiments were made to determine the best flow rate for the experiments. Slow flow rates may risk the adsorption of copper onto the walls of the glass syringe. Conversely, rapid flow rates do not allow the solution to heat up sufficiently before entering the column causing a significant temperature gradient. It was found that a flow rate of 200 ml/h was acceptable at lower temperatures (<50°C), however, this was decreased to 100 ml/h at higher temperatures to ensure that the solution reached the desired temperature. It was demonstrated by Mountain and Seward (1999) that the dissolution rate of chalcocite at room temperature is rapid and equilibration is reached even at flow rates of 1000 ml/h, therefore, experiments to test for equilibration at higher temperatures were considered unnecessary.

Hydrosulfide solutions were prepared using doubly-distilled and de-ionized water that was pH-adjusted using 1.0 mol/L NaOH. The solution flask was placed in an ultrasonic bath and evacuated for approximately 30 min to remove dissolved oxygen from the solution. The room temperature solubility of reduced sulfur at neutral pH and room temperature is approximately 0.2 mol $kg^{-1}$. $H_2S$ solubility decreases with increasing temperature and a saturated solution begins to degas $H_2S$ as it is heated. To prevent large volumes of exsolved $H_2S$ gas from collecting in the column and exit syringe, mixtures of $H_2S/N_2$ were used to saturate the experimental solution. After the solution flask was connected to the injection stem, the entire flow path was evacuated up to the column. Hydrosulfide solution was forced into the input syringe by imposing a slight overpressure of the appropriate gas mixture on the solution in the flask. This allows an approximately constant reduced sulfur concentration in the input solution. The rapid flow rate through the PVC tubing and column prevents loss of $H_2S$ and incursion of $O_2$ and the yellow coloration diagnostic of polysulfide formation due to sulfide oxidation was not observed. Highly reducing conditions due to the absence of oxygen and the presence of high concentrations of reduced sulfur ensures that all dissolved copper remains in the +1 oxidation state.

The room temperature pH of the solution was measured at the beginning of each experiment and then at equal intervals afterwards using a ROSS 8103 semimicro combination pH electrode connected to a Radiometer Copenhagen PHM 95 pH meter (± 0.05 pH units). It was considered too difficult to accurately measure the pH at temperature inside the oven and consequently experimental pH was calculated (see below). In early experiments, iodometric titrations for total reduced sulfur (±0.8%) were made on aliquots of the entering solution collected at the injection stem as well as on an aliquot of the effluent. No significant difference was found between these values indicating that no change in total reduced sulfur occurred during passage through the column. It was considered sufficient in the remaining experiments to measure reduced sulfur in aliquots of the effluent. The remaining effluent was injected into an ultraclean glass flask to which a small amount of ultrapure HCl was added and the solution was purged of $H_2S$ using oxygen-free $N_2$. The solutions were taken to dryness after which approximately 1.5 ml of ultrapure aqua regia was added. The solutions were heated again to dryness and the residue taken up with 3% ultrapure HCl. Copper was analyzed by flame atomic absorption spectroscopy on a Varian 840A spectrometer using standard solutions matrix-matched with ultrapure NaCl and ultrapure 3% HCl. The large volume of sample allowed concentration of low level solutions and resulted in a maximum analytical uncertainty of approximately ±2% for copper. Sodium was analyzed by flame emission spectroscopy (±2%). The contribution of these uncertainties to the uncertainty in individual log $K_{Cc}$ estimates for each sample is much smaller than the overall range of log $K_{Cc}$ for each experiment (see below), consequently these errors were not considered further.

## 3. RESULTS AND DISCUSSION

### 3.1. Cumulative Stability Constant of $Cu(HS)_2^-$ at Elevated Temperatures

The stoichiometries of hydrosulfide complexes of any metal are determined by the concentration of total reduced sulfur and pH. As sulfur increases, the ligand number of the complex can also increase, while as pH rises, more $HS^-$ ligand becomes

available to form multi-ligand complexes. To determine complex stoichiometry, it is necessary to measure copper solubility at a number of different total reduced sulfur concentrations and pH values. Mountain and Seward (1999) undertook such a study in which chalcocite solubility was measured in 46 experiments at differing pH and total reduced sulfur concentration to unambiguously define the copper hydrosulfide stoichiometries. In this study, it was considered unnecessary to redetermine the stoichiometry of the complex over the temperature range covered for two reasons; all measurements were made at near-neutral pH where $Cu(HS)_2^-$ is dominant and, because both $CuHS^o$ and $Cu(HS)_2^-$ stability constants are expected to change gradually with increasing temperature, it is unlikely that $CuHS^o$ would become the dominant complex over the temperature range studied. Any unusual change in shape of the solubility curve with increasing temperature could signify a change in complex stoichiometry, however, none was observed and $Cu(HS)_2^-$ is concluded to be the dominant complex in our experiments.

Table 1 lists the data from twelve flow through experiments spanning the temperature range of 35–95°C at approximate 10°C intervals. In all experiments, a slight temperature gradient occurred between the ends of the column (<3°C) so the listed temperature represents the average of the T3 and T5 thermocouples (Fig. 1). The pH values shown are in situ values calculated using the compositional data from the samples. In Figure 2, the results from one such experiment are plotted equidistant by sample number. The copper concentration is reproducible over the duration of the experiment giving a high degree of reliability in the calculated constants. This is important because the change in the stability constant of $Cu(HS)_2^-$ with each 10°C increase in temperature is small. The continuous increase in total sulfur with increasing sample number is caused by an undersaturation of the solution at the beginning of the experiment that diminished as the experiment continued. At first glance, it would appear that copper remains constant while reduced sulfur increases, however, an increase in reduced sulfur also causes a decrease in pH thus the effects tend to cancel.

In general form, the solubility of chalcocite as hydrosulfide/sulfide complexes can be expressed by the reaction

$$\frac{x}{2}Cu_2S(s) + \left(y - \frac{x}{2}\right)HS^- = Cu_xS_yH_z^{x+z-2y} + \left(y - z - \frac{x}{2}\right)H^+ \quad (1)$$

This reaction includes all complexes of the cuprous cation with any combination of sulfur and hydrogen ion, including polynuclear species (x>1). This can be simplified because only the $Cu(HS)_2^-$ complex (x = 1, y = z = 2) is being considered, reducing Eqn. 1 to

$$0.5Cu_2S(s) + 1.5HS^- + 0.5H^+ = Cu(HS)_2^- \quad (2)$$

whose logarithmic mass action expression is

$$log\ K_{Cc} = log\ a_{Cu(HS)_2^-} - 1.5log\ a_{HS^-} + 0.5\ pH \quad (3)$$

assuming the activity of $Cu_2S(s)$ to be unity. If the $Cu(HS)_2^-$ and $HS^-$ activities and pH are known, Eqn. 3 can be used to calculate log $K_{Cc}$ at any conditions. Note that the pH used must be the experimental pH at temperature and not the room temperature pH of the entering solution. This requires either measurement of pH in situ during the experiment or calculation of experimental pH from input solution composition. Although the former is desirable, it is experimentally difficult with the current apparatus and the latter approach was taken.

Experimental pH values were determined using the equilibrium solver program EQBRMB, a modification of a program given in Anderson and Crerar (1993). The program calculates the activities of species in $NaOH\text{-}H_2S\text{-}H_2O$ solutions using the total sulfur and total sodium concentrations as the input data. Activity coefficients were calculated using the modified Debye-Huckel equation (Helgeson, 1969). The value of å for $Cu(HS)_2^-$ was assumed to be 4.0. The necessary equilibria at each temperature include the first dissociation constants of $H_2S$ (Suleimenov and Seward, 1997), the dissociation constants of $NaOH^o$ (Ho and Palmer, 1996), and the dissociation constants of $NaHS^o$ (assumed to be equal to those of the $NaCl^o$ ion pair). Using the calculated in situ pH, $a_{HS^-}$, and the copper concentration, a measure of the equilibrium constant, $K_{cc}$, can be determined for each sample at their respective temperatures.

The calculated $K_{Cc}$ values for each sample are listed in Table 1 and plotted versus sample number in Figure 3 where lines connect isothermal estimates of the equilibrium constant of Eqn. 2 based on each measured copper and sulfur concentration and calculated pH. The straight dashed line represents the equilibrium constant measured at room temperature by Mountain and Seward (1999). Although some discrepancies are apparent, the results show a general increase in the equilibrium constants with increasing temperature. As stated above, only a minor part of the scatter in each experiment can be due to analytical uncertainties in sodium, copper and sulfur concentrations and most is attributed to the imprecision of the solubility method. The vertical range of Figure 3 should be noted, i.e., the entire set of results spans only about one logarithmic unit. Table 1 also lists the average, median and standard deviation of the results for each experiment. The median value of $K_{Cc}$ for each experiment was chosen to represent the equilibrium constant at that temperature rather than the average since the latter is sensitive to outliers (in most cases there was no significant difference between these statistics). One standard deviation was used to represent the spread (Fig. 4). At room temperature, the measured log $K_{Cc}$ is −0.13 (Mountain and Seward, 1999) while at 95°C the value is +0.55. Thus, these experiments have successfully measured a change of only 0.7 logarithmic units or a five-fold increase in $K_{Cc}$ as temperature increases. This represents an average change in log $K_{Cc}$ of only 0.1 logarithmic units for every 10°C temperature increase.

The experimental results are plotted in Figure 4 with the room temperature value of Mountain and Seward (1999) and the high temperature results of Crerar and Barnes (1976). The data below 100°C represent experimentally measured stability constants and are free of any extrapolation methods. These constants can be used to determine the solubilities of any copper mineral as $Cu(HS)_2^-$ by substitution of the appropriate mineral reaction involving that mineral and chalcocite. The stability constants above 100°C were derived from the solubility data of Crerar and Barnes (1976) who measured copper solubility in equilibrium with chalcopyrite-bornite. Mountain and Seward (1999) refit these data, using the $CuHS^o$ and

Table 1. The solubility of $Cu_2S$ as ΣCu ($\mu$g $kg^{-1}$) at temperature (°C), ΣS (mol $kg^{-1}$), in situ pH and the resultant $K_{Cc}$.

| | °C | ΣS | pH | ΣCu | $K_{Cc}$ |
|---|---|---|---|---|---|
| | 35.7 | 0.152 | 6.65 | 505 | 1.08 |
| | 36.3 | 0.152 | 6.65 | 471 | 1.12 |
| | 34.7 | 0.152 | 6.65 | 477 | 1.04 |
| | 35.7 | 0.157 | 6.63 | 493 | 1.03 |
| | 34.5 | 0.157 | 6.63 | 516 | 1.08 |
| | 36.1 | 0.154 | 6.64 | 383 | 0.783 |
| | 35.8 | 0.154 | 6.64 | 468 | 0.998 |
| | 35.2 | 0.161 | 6.61 | 455 | 0.920 |
| Median | 35.7 | 0.154 | 6.64 | 474 | 1.03 |
| Average | 35.5 | 0.155 | 6.64 | 469 | 1.00 |
| 1$\sigma$ | | | | | 0.11 |
| | 35.7 | 0.0203 | 6.94 | 22 | 0.865 |
| | 36.2 | 0.0203 | 7.09 | 25 | 0.926 |
| | 36.1 | 0.0202 | 7.10 | 24 | 0.895 |
| | 35.7 | 0.0217 | 7.07 | 21 | 0.787 |
| | 36.0 | 0.0217 | 7.07 | 24 | 0.863 |
| | 35.4 | 0.0204 | 7.09 | 26 | 0.945 |
| | 35.4 | 0.0218 | 7.06 | 27 | 0.961 |
| Median | 35.7 | 0.0204 | 7.07 | 24 | 0.895 |
| Average | 35.8 | 0.0215 | 7.06 | 24 | 0.892 |
| 1$\sigma$ | | | | | 0.060 |
| | 45.2 | 0.158 | 6.52 | 777 | 1.45 |
| | 45.5 | 0.157 | 6.52 | 643 | 1.19 |
| | 44.7 | 0.157 | 6.52 | 567 | 1.05 |
| | 45.7 | 0.155 | 6.53 | 562 | 1.06 |
| | 45.5 | 0.155 | 6.53 | 577 | 1.09 |
| | 45.3 | 0.152 | 6.55 | 523 | 1.00 |
| | 45.1 | 0.152 | 6.55 | 532 | 1.00 |
| | 45.1 | 0.156 | 6.53 | 547 | 1.02 |
| | 45.1 | 0.156 | 6.53 | 574 | 1.08 |
| Median | 45.2 | 0.156 | 6.53 | 567 | 1.06 |
| Average | 45.3 | 0.155 | 6.53 | 585 | 1.11 |
| 1$\sigma$ | | | | | 0.14 |
| | 47.8 | 0.0185 | 7.13 | 17 | 0.697 |
| | 46.8 | 0.0185 | 7.13 | 20 | 0.818 |
| | 46.8 | 0.0181 | 7.16 | 22 | 0.893 |
| | 46.3 | 0.0187 | 7.11 | 20 | 0.787 |
| | 46.1 | 0.0181 | 7.16 | 21 | 0.858 |
| | 46.1 | 0.0186 | 7.12 | 21 | 0.833 |
| | 45.9 | 0.0188 | 7.10 | 23 | 0.856 |
| | 45.9 | 0.0188 | 7.10 | 23 | 0.960 |
| Median | 46.2 | 0.0186 | 7.12 | 21 | 0.845 |
| Average | 46.4 | 0.0185 | 7.13 | 21 | 0.838 |
| 1$\sigma$ | | | | | 0.077 |
| | 51.9 | 0.0201 | 6.92 | 48 | 1.48 |
| | 54.2 | 0.0189 | 7.00 | 35 | 1.18 |
| | 52.9 | 0.0200 | 6.92 | 39 | 1.18 |
| | 55.6 | 0.0200 | 6.92 | 41 | 1.27 |
| | 55.2 | 0.0198 | 6.94 | 47 | 1.48 |
| | 55.1 | 0.0208 | 6.87 | 40 | 1.14 |
| | 55.8 | 0.0206 | 6.88 | 57 | 1.67 |
| Median | 55.1 | 0.0200 | 6.92 | 41 | 1.27 |
| Average | 54.4 | 0.0200 | 6.92 | 42 | 1.34 |
| 1$\sigma$ | | | | | 0.20 |
| | 66.9 | 0.0164 | 7.20 | 46 | 1.96 |
| | 67.0 | 0.0164 | 7.20 | 51 | 2.20 |
| | 66.5 | 0.0163 | 7.22 | 44 | 1.91 |
| | 66.6 | 0.0168 | 7.14 | 49 | 1.97 |
| | 66.3 | 0.0168 | 7.14 | 48 | 1.93 |
| | 65.4 | 0.0171 | 7.11 | 58 | 2.22 |
| | 66.0 | 0.0174 | 7.07 | 47 | 1.73 |
| | 65.0 | 0.0176 | 7.05 | 45 | 1.61 |

Table 1. continued

| | °C | ΣS | pH | ΣCu | $K_{Cc}$ |
|---|---|---|---|---|---|
| Median | 66.4 | 0.0168 | 7.14 | 47 | 1.95 |
| Average | 66.2 | 0.0169 | 7.14 | 48 | 1.94 |
| 1$\sigma$ | | | | | 0.21 |
| | 64.4 | 0.0212 | 6.78 | 69 | 1.82 |
| | 66.7 | 0.0216 | 6.76 | 58 | 1.45 |
| | 65.6 | 0.0216 | 6.76 | 54 | 1.38 |
| | 67.1 | 0.0220 | 6.73 | 50 | 1.23 |
| | 67.5 | 0.0221 | 6.73 | 40 | 0.99 |
| | 68.5 | 0.0223 | 6.72 | 53 | 1.29 |
| | 66.8 | 0.0216 | 6.76 | 60 | 1.55 |
| Median | 66.8 | 0.0216 | 6.76 | 54 | 1.38 |
| Average | 66.6 | 0.0218 | 6.74 | 54 | 1.39 |
| 1$\sigma$ | | | | | 0.26 |
| | 76.0 | 0.0217 | 6.56 | 80 | 2.00 |
| | 76.9 | 0.0205 | 6.62 | 68 | 1.82 |
| | 77.9 | 0.0205 | 6.62 | 63 | 1.82 |
| | 76.1 | 0.0207 | 6.61 | 70 | 1.84 |
| | 77.6 | 0.0201 | 6.64 | 64 | 2.00 |
| | 75.8 | 0.0203 | 6.63 | 72 | 1.97 |
| | 77.5 | 0.0205 | 6.62 | 67 | 1.82 |
| | 76.9 | 0.0201 | 6.64 | 77 | 2.09 |
| Median | 76.9 | 0.0205 | 6.62 | 69 | 1.91 |
| Average | 76.8 | 0.0206 | 6.62 | 70 | 1.92 |
| 1$\sigma$ | | | | | 0.11 |
| | 84.4 | 0.0883 | 6.90 | 934 | 2.74 |
| | 85.7 | 0.0883 | 6.90 | 1165 | 3.39 |
| | 83.2 | 0.0797 | 7.13 | 1276 | 4.81 |
| | 83.2 | 0.0834 | 7.01 | 894 | 2.96 |
| | 85.8 | 0.0816 | 7.06 | 1065 | 3.53 |
| | 86.3 | 0.0816 | 7.06 | 1065 | 7.45 |
| | 86.3 | 0.0816 | 7.06 | 1324 | 1.93 |
| Median | 85.7 | 0.0816 | 7.06 | 1065 | 3.39 |
| Average | 84.0 | 0.0835 | 7.02 | 1093 | 3.83 |
| 1$\sigma$ | | | | | 0.19 |
| | 86.2 | 0.0159 | 6.71 | 83 | 2.46 |
| | 87.4 | 0.0163 | 6.90 | 73 | 2.69 |
| | 86.9 | 0.0170 | 6.86 | 75 | 2.63 |
| | 85.8 | 0.0171 | 6.80 | 77 | 2.51 |
| | 85.6 | 0.0168 | 6.79 | 79 | 2.61 |
| | 86.2 | 0.0173 | 6.78 | 67 | 2.13 |
| | 89.2 | 0.0172 | 6.78 | 51 | 1.63 |
| | 83.7 | 0.0168 | 6.82 | 64 | 2.13 |
| Median | 86.2 | 0.0169 | 6.80 | 74 | 2.48 |
| Average | 86.4 | 0.0168 | 6.80 | 70 | 2.35 |
| 1$\sigma$ | | | | | 0.36 |
| | 95.5 | 0.0788 | 7.14 | 477 | 3.08 |
| | 95.5 | 0.0743 | 7.36 | 924 | 4.57 |
| | 95.5 | 0.0786 | 7.14 | 629 | 2.47 |
| | 95.5 | 0.0716 | 7.58 | 775 | 5.00 |
| Median | 95.5 | 0.0765 | 7.25 | 698 | 3.82 |
| Average | 95.5 | 0.0758 | 7.31 | 681 | 3.78 |
| 1$\sigma$ | | | | | 1.20 |
| | 94.7 | 0.0188 | 6.82 | 125 | 3.52 |
| | 91.8 | 0.0189 | 6.82 | 98 | 2.71 |
| | 92.1 | 0.0203 | 6.72 | 120 | 3.04 |
| | 97.2 | 0.0188 | 6.82 | 124 | 3.52 |
| | 93.7 | 0.0177 | 6.93 | 126 | 4.05 |
| | 93.8 | 0.0188 | 6.82 | 124 | 3.52 |
| | 94.2 | 0.0185 | 6.85 | 108 | 3.16 |
| | 94.8 | 0.0189 | 6.82 | 113 | 3.18 |
| Median | 94.0 | 0.0188 | 6.82 | 122 | 3.35 |
| Average | 94.0 | 0.0188 | 6.82 | 116 | 3.34 |
| 1$\sigma$ | | | | | 0.40 |

$Cu(HS)_2^-$ species, and determine estimates for log $K_{Cc}$ by subtracting the mineral reaction between chalcopyrite, bornite and chalcocite. It can be seen in Figure 4 that there is a continuous upward curving trend from 25 to 300°C suggesting that the results represent a single equilibrium. The curvature of the data shows that the enthalpy of Eqn. 2 is positive and increases with increasing temperature. This curvature is the result of the dissolution/complexation reaction being nonisocoulombic. In isocoulombic reactions, where a equal number of like charges are found on both sides of the reaction, effects on dissolved species heat capacities due to ion-solvent interactions tend to cancel resulting in a near constant and near zero $\Delta C_p$ with increasing temperature (Mesmer and Baes, 1974; Lindsay, 1980).

For the purposes of geochemical modeling, the value of the cumulative stability constant of $Cu(HS)_2^-$ (log $\beta_{122}$) over a range of temperatures is the most useful parameter that can be incorporated into a thermodynamic database. This allows the inclusion of $Cu(HS)_2^-$ into simulations of copper transport and deposition. The $Cu(HS)_2^-$ complexation reaction is represented by:

$$Cu^+ + 2HS^- = Cu(HS)_2^-. \quad (4)$$

In order to derive values for the stability constant of this reaction from the data in Figure 4, it is necessary to subtract the chalcocite dissolution reaction

$$0.5\ Cu_2S + 0.5H^+ = Cu^+ + 0.5HS^- \quad (5)$$

from Eqn. 2. In the ideal case, thermodynamic data for all species in Eqn. 5 would be available, however, the lack of thermodynamic data for the cuprous cation at elevated temperatures precludes a purely experimental derivation of the cumulative stability constant of $Cu(HS)_2^-$. It is therefore necessary to obtain the equilibrium constant of the chalcocite dissolution reaction using predictive methods. Equilibrium constants for the mineral reaction were calculated using SUPCRT92 (Johnson et al., 1992) and adjusted using the experimental determination of the first dissociation constant of $H_2S$ of Suleimenov and Seward (1997). Figure 5 shows the corresponding cumulative stability constants for Eqn. 4 calculated for each experiment by subtracting the equilibrium constant for the chalcocite dissolution reaction from that of Eqn. 2. The downward trend of log $\beta_{122}$ is due to a negative enthalpy of complexation that is typical of soft cation-soft anion interaction at lower temperatures. At higher temperature (>150°C), the enthalpy of complexation begins to approach zero as cation-anion interactions become more electrostatic and reaches zero at ~275°C. Above this temperature, cation-anion interactions are more electrostatic, hard-hard interactions (Seward, 1981). The change of $\Delta H$ from negative to positive results in the upward curvature of log $\beta_{122}$.

The evaluation of the thermodynamic functions from equilibrium constants requires the statistical fitting of some form of algebraic expression to the experimental log $\beta_{122}$ values. The curvature of the measured log $\beta_{122}$ implies that the enthalpy of the reaction is not constant and therefore a simple van't Hoff equation is not appropriate in this case, at least at temperatures above ~100°C. The most convenient form of equation expresses the equilibrium constant of the reaction as a function of temperature in which the desired standard state thermodynamic values are the fitting parameters. As log $\beta$ is a smooth function of temperature, its value can be expressed as a perturbation on the value of ln $\beta_\theta$ at reference temperature using a Taylor series expansion (Clark and Glew, 1966). Using this approach, a continuous function is obtained with the form

$$ln\beta_T = ln\beta^\circ_\theta + \frac{\Delta H^\circ_\theta}{R}t_1 + \frac{\Delta C^\circ_{p\theta}}{R}t_2 + \frac{\theta}{2R}\frac{d\Delta C^\circ_{p\theta}}{dT}t_3 + \frac{\theta^2}{12R}\frac{d^2\Delta C^\circ_{p\theta}}{dT^2}t_4 + \frac{\theta^3}{72R}\frac{d^3\Delta C^\circ_{p\theta}}{dT^3}t_5 \quad (6)$$

where

$$t_1 = \left[\frac{1}{\theta} - \frac{1}{T}\right]$$

$$t_2 = \left[\left(\frac{\theta}{T}\right) - 1 + 1n\left(\frac{T}{\theta}\right)\right]$$

$$t_3 = \left[\left(\frac{T}{\theta}\right) - \left(\frac{\theta}{T}\right) - 2ln\left(\frac{T}{\theta}\right)\right]$$

$$t_4 = \left[\left(\frac{T}{\theta}\right)^2 - 6\left(\frac{T}{\theta}\right) + 3 + 2\left(\frac{\theta}{T}\right) + 6ln\left(\frac{T}{\theta}\right)\right]$$

$$t_5 = \left[\left(\frac{T}{\theta}\right)^3 - 6\left(\frac{T}{\theta}\right)^2 + 18\left(\frac{T}{\theta}\right) - 10 - 3\left(\frac{\theta}{T}\right) - 12ln\left(\frac{T}{\theta}\right)\right].$$

Eqn. 6 is arbitrarily terminated after the sixth term since inordinately accurate experimental data would be required to obtain meaningful higher order derivatives of $\Delta C_p^\circ$. The experimental values of log $\beta_{122}$ were fit using Eqn. 6 with the program STATGRAPHICS 3.1 to obtain the nonlinear regression line shown in Figure 5 and the necessary fitting parameters for Eqn. 6. These were used to calculate the cumulative stability constants for $Cu(HS)_2^-$ at the temperatures listed in Table 2 and, in turn, the pertinent thermodynamic parameters at 298 K (Table 3).

### 3.2. Comparison with Theoretical Extrapolations

We have applied two extrapolation techniques to the low temperature data to obtain estimates of the high temperature stability constants of $Cu(HS)_2^-$; a two-term isocoulombic extrapolation using our low temperature data and the one-term isocoulombic extrapolation of Gu et al. (1994). As mentioned above, an isocoulombic reaction is one in which the number and charge of charged species is identical on both sides of the reaction. Reactions of this type tend to have near zero heat capacity change and thus have constant enthalpy with increasing temperature. Eqn. 4 can be written isocoulombically by the addition of another reaction that has well-known thermodynamic properties, in this case, the $H_2S$ dissociation reaction

$$H_2S(aq) = HS^- + H^+. \quad (7)$$

Addition of Eqns. 4 and 7 results in the isocoulombic reaction

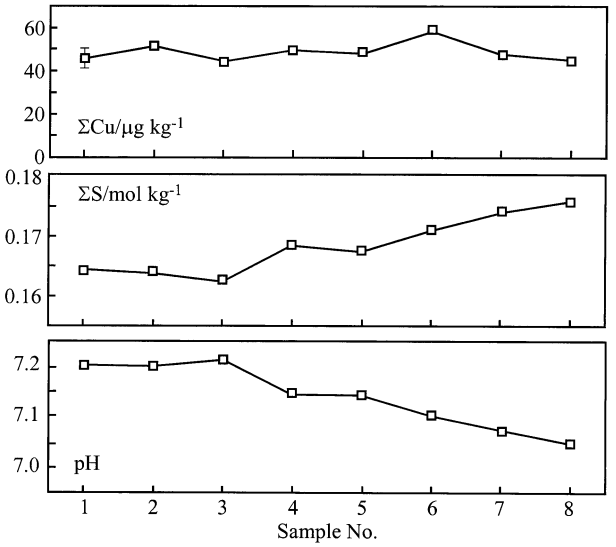


Fig. 2. An example of results from a flow through experiment conducted at approximately 65°C showing reproducible copper concentrations (Cu/($\mu$g kg$^{-1}$). Hydrogen sulfide concentration increases slightly over the experiment causing the decrease in pH.

$$Cu^{+} + H_2S(aq) + HS^{-} = Cu(HS)_2^{-} + H^{+}. \quad (8)$$

The dissociation constants for Eqn. 7 between 25 and 100°C were obtained using the equation of Suleimenov and Seward (1997) and added to the values of log $\beta_{122}$ obtained in this study. Assuming that the $\Delta C_p$ of the Eqn. 8 is zero, the log K of this reaction can be extrapolated to high temperature if stability constants are available at two temperatures. We have used a simple linear regression of the low temperature data to obtain the solid line shown in Figure 6. A comparison of the extrapolation with the constants derived previously and adjusted using the $H_2S$ dissociation reaction shows perfect agreement up to 300°C. At 350°C there is a small discrepancy, however, considering the uncertainty in the slope of the regression line, the overall the agreement is excellent. Thus, two-term isocoulombic extrapolations give reasonable estimates of metal-ligand complex stabilities for soft metal–soft ligand interactions, such as the copper hydrosulfide example discussed here. Such extrapolations are highly useful in estimating stability constants of other soft metals such as silver, gold, thallium, mercury and the platinum group elements (cf. Mountain and Wood, 1988).

The one-term isocoulombic method of Gu et al. (1994) is based on the observation that for many isocoulombic reactions the $\Delta C_p$ and $\Delta S$ of reaction are both small and often opposite in sign thereby causing changes in the enthalpy and entropy terms of the free energy expression to cancel as temperature increases. This results in a relatively constant free energy of reaction with temperature, i.e.,

$$\Delta G_T = \Delta G_{T_0} = -RT \ln K_T, \quad (9)$$

and makes extrapolation of equilibrium constants to higher temperatures simple when compared with other methods. The one-term method was applied to Eqn. 8 using its free energy change at 25°C to obtain estimates of log $\beta_{122}$ + log $K_{H_2S}$ up

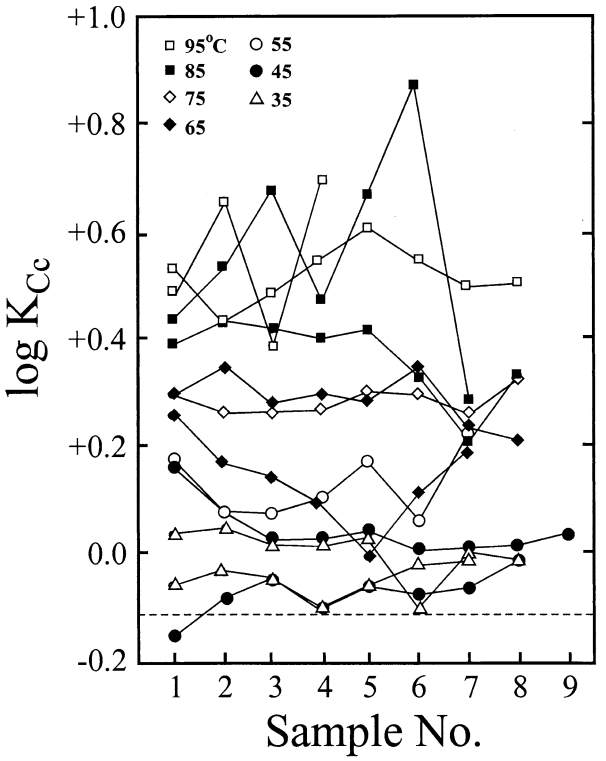


Fig. 3. Calculated log $K_{Cc}$ values for Eqn. 3 based on measured copper concentration, measured hydrogen sulfide concentration and calculated pH. Although some scatter is present, there is a general increase in log $K_{Cc}$ with increasing temperature.

to 350°C (Fig. 6). The resulting line progressively deviates from the values derived from experimental data and the previous two-term extrapolation as temperature increases. The maximum deviation from the measured data is ~1.2 log units at 350°C. This level of uncertainty is unacceptable for stability constant determinations using experimental data and the use of this method to predict such constants at high temperature should be done with caution. Gu et al. (1994) point out that the best isocoloumbic reactions are those which have the fewest energetic, electrostatic, volumetric and structural differences between reactants and products. Considering the form of Eqn. 8, it is evident that the volumetric and structural properties of the species are not balanced. A significant negative entropy change for this reaction would result in a positive departure of the one-term extrapolation (where $\Delta S$ is assumed to be zero) with increasing temperature. The entropy change of Eqn. 8 at 25°C is −16.4 cal/K giving a possible explanation for the discrepancy. Because the two-term extrapolation described previously is made using data at different temperatures, this entropy change is taken partially into consideration and the agreement is superior. Further discussion regarding the validity of the one-term method can be found in Wood and Samson (1998).

The room temperature stability constant of $CuHS^{o}$ was estimated by Mountain and Seward (1999) using a linear free energy relationship because low solubilities in the acid region prevented an experimental determination. Nonetheless, they were able to confirm the presence, and calculated the stability,

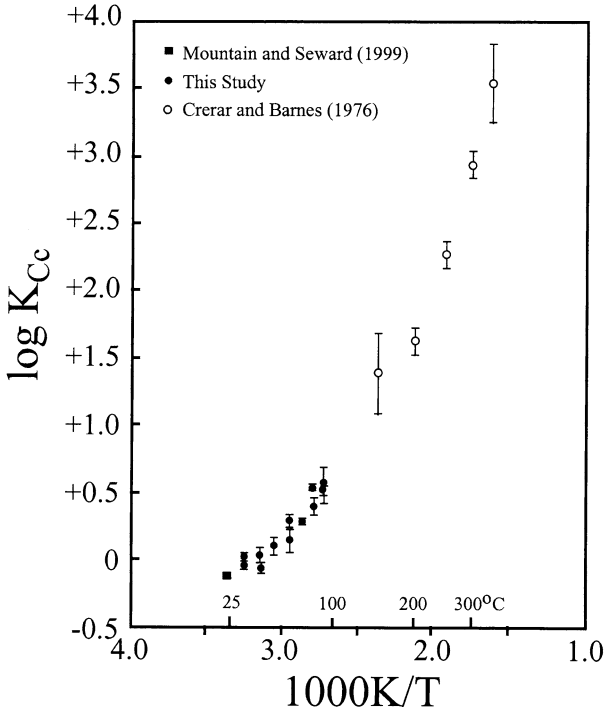


Fig. 4. Log $K_{Cc}$ from Eqn. 3 plotted as a function of inverse temperature (1000K/T). A positive curvature with increasing temperature indicates a positive and increasing enthalpy of reaction for Eqn. 2.

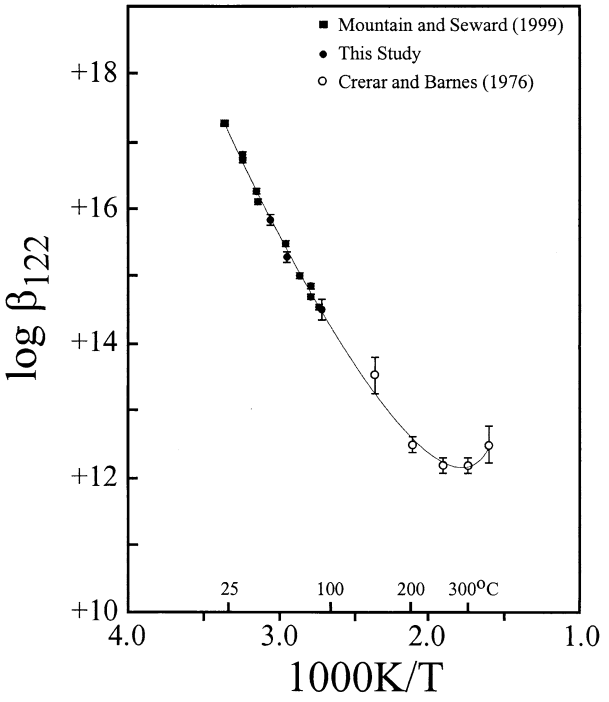


Fig. 5. Log $\beta_{122}$ for the $Cu(HS)_2^-$ complexation reaction plotted as a function of inverse temperature (1000K/T). These values were obtained by subtracting the log K of the chalcocite dissolution reaction, obtained using SUPCRT92 (Johnson et al., 1992) from that of Eqn. 3. The solid line represents the fit using the method of Clark and Glew (1966). The stability of the $Cu(HS)_2^-$ complex decreases substantially with temperature, however, it flattens out at ~275°C and then begins to increase.

of the $CuHS^o$ complex based on the experimental data of Crerar and Barnes (1976) at higher temperature (200–300°C). It is an interesting exercise to test the room temperature estimate by making an isocoulombic extrapolation down temperature to 25°C and compare it with the experimental result. The $CuHS^o$ complexation reaction can be made isocoulombic by the addition of the $H_2S$ dissociation reaction to give:

$$Cu^+ + H_2S(aq) = CuHS^o + H^+. \quad (10)$$

Simple linear regression of the three data points between 200 and 300°C allows extrapolation to room temperature and, by subtraction of the $H_2S$ reaction, gives the stability constant of $CuHS^o$ at this temperature. The resulting constant of log $\beta_{111}$ = +17 is four orders of magnitude higher than the estimate of +13 of Mountain and Seward (1999). This higher value is not supported by experimental evidence for two reasons. Firstly, such a high constant would have made experimental solubilities in the acid region easily measurable and, secondly, this value is essentially the same as the stability constant of $Cu(HS)_2^-$ (+17.2) which is unusual for stepwise cumulative stability constants for strong soft metal–soft ligand interactions. In the following calculations we have therefore retained the estimate for log $\beta_{111}$ determined in the earlier study.

### 3.3. Transport of Copper in Hydrothermal Solutions

The dominant ligands responsible for copper transport in hydrothermal fluids are chloride and hydrosulfide, with the former normally present at concentrations of one to two orders of magnitude higher than the latter (Seward and Barnes, 1997). This implies that copper transport in all hydrothermal fluids would be dominated by chloride complexes at all conditions. This is not always the case as the stabilities of the copper hydrosulfide complexes are several orders of magnitude higher than those of copper chloride complexes (Xiao et al., 1998; Mountain and Seward, 1999). In addition, the temperature dependence of their stability constants differs markedly. In a cooling hydrothermal fluid, chloride complex stability drops so dramatically, that extremely efficient deposition of chloride-complexed copper would occur, especially if water-rock interaction results in a simultaneous increase in pH. In contrast, hydrosulfide complex stability increases with decreasing temperature and a rise in pH can actually increase copper solubility as hydrosulfide complex. With the acquisition of high temperature stability constants for copper hydrosulfide and chloride complexes it is possible to determine under which physicochemical conditions one group of complexes will dominate.

Figure 7 shows the speciation of copper(I) as a function temperature, chloride activity, and hydrosulfide activity. Note that the activity of $HS^-$ is dependent on pH, thus at 25°C and neutral pH, log $a_{HS^-}$ is equal to about half the total sulfur concentration. At ambient temperature, the fields of $CuCl_3^{2-}$ and $CuCl_2^-$ are restricted to regions of low hydrosulfide activity ($<10^{-5}$) and high chloride activity ($>10^{-1}$). Up to ~150°C, the dominant complexes of copper(I) are expected to be $CuHS^o$ and/or $Cu(HS)_2^-$ at hydrosulfide activities above

Table 2. Cumulative stability constant (±95% confidence interval) for $Cu(HS)_2^-$ from 25 to 350°C calculated using Eqn. 6.

| T/°C | log $\beta_{122}$ |
|---|---|
| 25 | 17.3 ± 0.2 |
| 50 | 16.0 ± 0.2 |
| 100 | 14.4 ± 0.2 |
| 150 | 13.4 ± 0.2 |
| 200 | 12.6 ± 0.2 |
| 250 | 12.2 ± 0.2 |
| 300 | 12.1 ± 0.2 |
| 350 | 12.5 ± 0.3 |

Table 3. Thermodynamic functions (±95% confidence interval) for Eqn. 4 reference temperature $\theta = 298$ K.

| | | |
|---|---|---|
| ΔG° | −98.6 ± 0.3 | kJ $mol^{-1}$ |
| ΔH° | −102 ± 7 | kJ $mol^{-1}$ |
| ΔCp° | +0.80 ± 0.30 | kJ $mol^{-1}$ $K^{-1}$ |
| ΔS° | −11.1 | J $mol^{-1}$ |
| dΔCp°/dT | −11 ± 5 | J $mol^{-1}$ $K^{-2}$ |
| $d^2\Delta Cp°/dT^2$ | 0.09 ± 0.03 | J $mol^{-1}$ $K^{-3}$ |

$10^{-3}$ at all geologically reasonable chloride activities ($>10^{-2}$). As temperature is increased further, the fields of the chloride complexes expand at the expense of the hydrosulfide complexes pushing them to higher hydrosulfide activities and lower chloride activities. This is evident on the front faces of the diagram in Figure 7. At 300°C, only in solutions with hydrosulfide activities in excess of $\sim 10^{-3}$ would $Cu(HS)_2^-$ dominate and then only if chloride activity is less than $10^0$. These would be rare solutions as most silicate-buffered pH values would be well below the pH of the equal activity line for $H_2S^o/HS^-$ at 300°C (pH ~ 8).

The purpose of measuring metal complex stabilities is to allow us to model the transport and deposition of metals in hydrothermal solutions. This can be accomplished through the application of numerical models of metal transport both simple and complex and, if they are to be accurate, require confidence in our choice of complex stoichiometries and stabilities. We can examine the roles of both chloride and hydrosulfide complexing of copper in ore-forming systems using the derived stability constants. Although both types of complexes could be expected to be present in all copper ore-forming situations, significant concentrations of copper as chloride complexes are only possible at less than neutral pH values, high salinity or highly oxidizing conditions. An example where low pH solutions are responsible for the formation of economic copper mineralization is in high sulfidation epithermal deposits. In these deposits Cu-Au mineralization is hosted in highly altered host rock composed of vuggy silica commonly bounded by a zone of advanced argillic alteration containing typically quartz, kaolinite and alunite. This mineral assemblage is attributed to extensive alteration by highly acidic, low to intermediate salinity fluids that resulted from the condensation of a magmatic vapor into local meteoric water (Arribas, 1995).

Figure 8a shows contours for the solubility of copper in equilibrium with chalcocite, covellite and native copper. $CuCl_2^-$ is chosen to represent total solubility as chloride complexes based on the activity of free chloride at the indicated salinity (Fig. 7). The typical copper mineral encountered in high sulfidation deposits is enargite (Arribas, 1995) but the absence of data on the arsenic content of these fluids precludes calculation of enargite solubility. Covellite is also found in some cases and we use it as a proxy for enargite. The stability field of covellite is small and restricted to low pH, although it would expand if total sulfur content were greater. If, for example, a fluid with a pH ~ 2 was in equilibrium with covellite along the $H_2S/HSO_4^-$ equal activity line (Point A, Fig. 8a), $CuCl_2^-$ activity would reach approximately $10^{-2}$ or ~1500 mg $kg^{-1}$ (using appropriate activity coefficients at these conditions). At the same conditions, the solubility of covellite as $CuHS^o$ is only ~0.2 mg $kg^{-1}$ and as $Cu(HS)_2^-$, it is insignificant. Figure 8 shows that high concentrations of copper are necessary and perhaps geologically unrealistic, if mineralization is formed at extremely low pH. This would explain why the highest grade copper mineralization appears to be later than its vuggy silica host. Although fluid pH may have been low enough to form intense vuggy silica alteration, saturated copper concentrations are so high that the fluid probably remains undersaturated and only cooling or fluid neutralization could induce copper precipitation.

The advanced argillic zone, with an assemblage of kaolinite-alunite-muscovite-quartz, is not stable at pH < 2.5 unless unreasonably high potassium concentrations are present. If the previous fluid equilibrated with this assemblage (Point B, Fig. 8a), copper solubility drops to ~300 mg $kg^{-1}$ as water-rock interaction occurs and pH rises. Copper solubility as $CuHS^o$ decreases to 0.1 mg $kg^{-1}$. If the resulting fluid reacts further to form a phyllic alteration assemblage and eventually equilibrates with potassium feldspar-muscovite-quartz-chalcocite (along the $HSO_4^-/H_2S$ equal activity line), copper solubility as chloride complexes drops to ~3 mg $kg^{-1}$ (Point C, Fig. 8a). At the same time, solubility of copper as $CuHS^o$ remains essentially unchanged and thus is unlikely to play a significant role in copper mineralization formed in distal alteration zones in high sulfidation deposits. The above reaction path is isothermal; decreasing temperature would further destabilize chloride complexes and stabilize hydrosulfide complexes. Copper solubility as $Cu(HS)_2^-$ reaches a maximum at pH ~ 8 (up to ~2 mg $kg^{-1}$) at 300°C (Point D, Fig. 8a). It is clear that in high sulfidation epithermal deposits, hydrosulfide complexes of copper cannot contribute significantly to the main mineralization unless considerably higher sulfur activities are present. The high copper concentrations attainable as chloride complexes, even at relatively low salinities, also indicate that relatively low water/rock ratios are required to form significant copper mineralization.

In low sulfidation epithermal deposits, mineralization is found as low sulfidation state sulfides such as pyrite, sphalerite and chalcopyrite. The fluids responsible for their formation are considered to be analogous to those found in many active geothermal systems, being relatively reducing, near neutral in pH and of low salinity (Henley and Ellis, 1983; Hedenquist and Henley, 1985). Mountain and Seward (1999) have shown that in a typical Broadlands geothermal fluid, all copper transport occurs as hydrosulfide complexes.

Figure 8b shows the solubility of chalcopyrite and bornite as copper chloride and hydrosulfide complexes in a fluid with total chloride content of 1.0 mol $kg^{-1}$ and a total sulfur of 0.01 mol

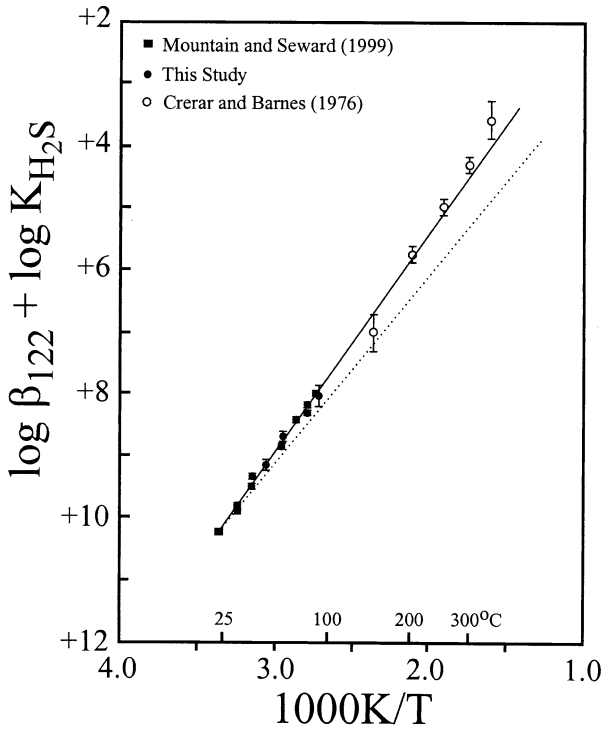


Fig. 6. Log K values for the isocoulombic reaction composed of the combination of log $\beta_{122}$ for the $Cu(HS)_2^-$ complexation reaction and the first dissociation constant of $H_2S$(aq) plotted as a function of inverse temperature (1000K/T). If this reaction is truly isocoulombic then its heat capacity change is zero and the enthalpy is a constant. This allows extrapolation to higher temperature using at least two measured values at different temperatures. The solid straight line represents a two-term isocoulombic extrapolation based on the linear regression of values below 100°C. The agreement with the estimated values from Mountain and Seward (1999), based on the data of Crerar and Barnes (1976), is excellent. The dashed line represents a one-term isocoulombic extrapolation based on the method of Gu et al. (1994).

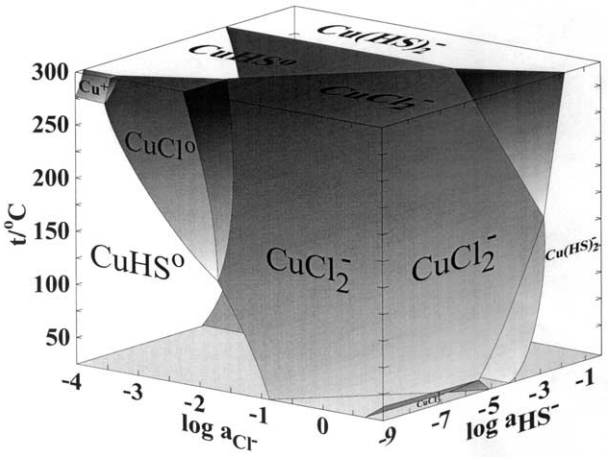


Fig. 7. Three-dimensional speciation diagram showing the predominance fields of the copper chloride and hydrosulfide complexes as a function of temperature, chloride, and $HS^-$ activity. At low temperature, the fields of the copper chloride complexes are small and restricted to high chloride activities (>0.1). As temperature increases, the fields of the copper chloride complexes expand substantially. At 300°C, in most geologically relevant solutions, $CuCl_2^-$ will be the dominant complex of copper with hydrosulfide complexes important only when hydrosulfide activity is high.

$kg^{-1}$. It can be seen that under acid conditions such as would be encountered in equilibrium with kaolinite-muscovite-quartz (KAM), significant copper concentrations are possible as chloride complexes. In equilibrium with potassium feldspar-muscovite-quartz (KFM) copper concentrations as chloride and hydrosulfide complexes are low when in equilibrium with chalcopyrite. Significant solubilities are possible at the slightly alkaline pH values near the $H_2S/HS^-$ equal activity line where copper solubility as hydrosulfide complexes reaches around 2 mg $kg^{-1}$ (Point E, Fig. 8b). In this region, chloride complexation is insignificant and unreasonably high salinities would be required to transport enough copper to match that of the hydrosulfide complexes, thus in low sulfidation deposits, $Cu(HS)_2^-$ is could be expected as the dominant copper complex.

Although copper solubility as $CuHS^o$ and $Cu(HS)_2^-$ clearly does not reach the high concentrations possible as chloride complexes (at low pH), it may be enough to play a significant role in forming anomalous copper mineralization. Copper mineralization in other ore deposit types, where high sulfur activities and neutral to alkaline pH values occur (e.g., mesothermal gold deposits and hydrothermal deposits in ultramafic rocks), would also be expected to be the result of copper transport as hydrosulfide complexes.

## 4. CONCLUSIONS

The solubility of $Cu_2S$ has been measured in sulfide-bearing solutions of near neutral pH up to 95°C. These data were collected to confirm the high temperature stability constants for $Cu(HS)_2^-$ up to 350°C previously estimated by Mountain and Seward (1999) from the solubility data of Crerar and Barnes (1976). Isocoulombic extrapolation allowed calculation of better estimates of these constants and these were found to agree closely with the earlier estimates. The new constants allow meaningful calculations for the solubility of copper minerals at high temperatures as hydrosulfide complexes.

Although chloride complexes are dominant under most conditions, their strong temperature dependence means that solubilities drop dramatically as temperature decreases. The opposite is true for hydrosulfide complexes whose stabilities increase substantially as temperature decreases. It is expected that at high temperatures and low pH, chloride complexes of copper will dominate copper solubilities and that the only hydrosulfide complex of significance will be $CuHS^o$ under these conditions. More neutral to alkaline pH values and reducing conditions favor complexation as $Cu(HS)_2^-$ and under these conditions the solubility of copper as chloride complexes will be subordinate. The relatively low solubilities of copper as hydrosulfide complexes under these conditions may explain why many low sulfidation epithermal deposits and geothermal systems, although anomalous in copper, are not greatly enriched. The results of this study provide the necessary thermodynamic data to construct more complete and reliable models of the processes involved in the generation of copper deposits.

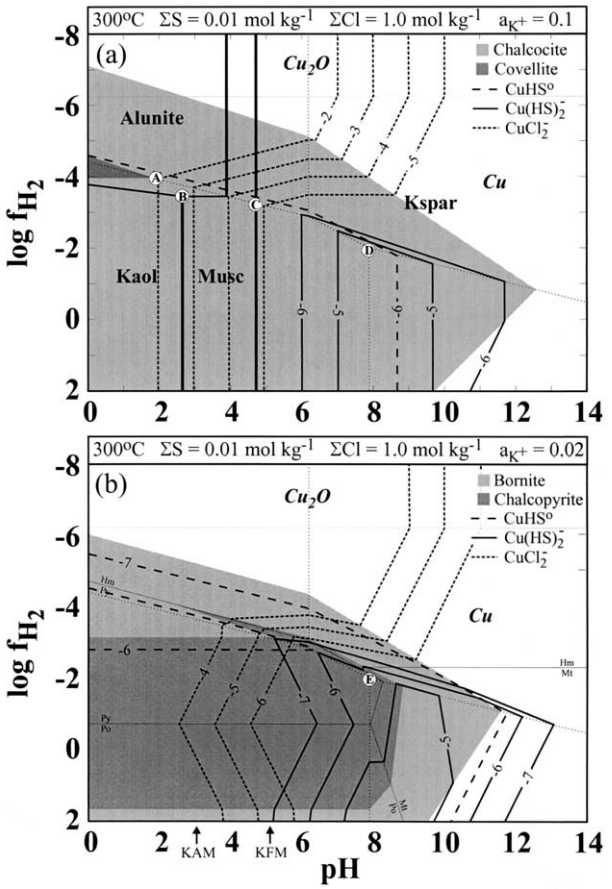


Fig. 8. Log $f_{H_2}$-pH diagrams showing solubility of copper minerals under physicochemical conditions representative of high and low sulphidation epithermal environments. (a) Chalcocite-covellite-Cu(s)-cuprite solubility shown as chloride and hydrosulfide complexes. Under the acidic and oxidizing conditions expected in high sulfidation environments, copper solubility as chloride complexes is high but measurable solubilities as $CuHS^o$ are possible. $Cu(HS)_2^-$ is not expected to contributed to total copper solubility under these conditions. (b) Chalcopyrite-bornite-Cu(s)-cuprite solubility shown as chloride and hydrosulfide complexes. Under the more neutral and reducing conditions of low sulfidation deposits, copper transport as chloride complexes is low and significant transport as $Cu(HS)_2^-$ is expected. Copper solubility as $Cu(HS)_2^-$ reaches its maximum at the $H_2S$-$HS^-$-$SO_4^{2-}$ triple point. Shaded areas represent stability fields of copper sulfides and thin solid lines separate stability fields of other mineral phases. Fe mineral stability fields are labeled on boundaries in (b). Dotted lines separate the predominance fields of the dissolved sulfur species. Heavy solid lines in (a) separate stability fields of aluminosilicates and alunite. Contoured copper solubilities are shown as short dashed lines ($CuCl_2^-$); solid lines ($Cu(HS)_2^-$), and long dashed lines ($CuHS^o$). KAM and KFM are the kaolinite-muscovite-quartz and potassium feldspar-muscovite-quartz pH buffers, respectively, at the indicated potassium activity. Points A–E are referred to in the text.

*Acknowledgments*—We thank our colleagues in Zurich, especially Oleg Suleimenov, for useful discussions. This study was completed at the Institute of Geological and Nuclear Sciences, Wairakei, New Zealand. We thank Artashes Migdisov and two anonymous reviewers for their helpful comments on the manuscript. BWM acknowledges the support of the New Zealand Foundation for Research in Science and Technology Contract No. C05X0004.

*Associate editor:* L. G. Benning

## REFERENCES

Anderson G. M. and Crerar D. (1993) *Thermodynamics in Geochemistry: The Equilibrium Model.* Oxford University Press.

Arribas A. Jr. (1995) Characteristics of high-sulfidation epithermal deposits, and their relation to magmatic fluid. *Mineral. Assoc. Can. Short Course* **23**, 419–454.

Bethke C. M. (1996) *Geochemical Reaction Modelling: Concepts and Applications.*Oxford University Press.

Clark E. C. W. and Glew D. N. (1966) Evaluation of thermodynamic functions from equilibrium constants. *Trans. Faraday Soc.* **62**, 539–547.

Crerar D. and Barnes H. (1976) Ore solution chemistry V. Solubilities of chalcopyrite and chalcocite assemblages in hydrothermal solutions at 200°C to 350°C. *Econ. Geol.* **71**, 772–794.

Gu Y., Gammons C. H., and Bloom M. S. (1994) A one-term extrapolation method for estimating equilibrium constants of aqueous reactions at elevated temperatures. *Geochim. Cosmochim. Acta* **58**, 3545–3560.

Hedenquist J. W. and Henley R. W. (1985) Hydrothermal eruptions in the Waiotapu geothermal system, New Zealand: Their origin, associated breccias and relation to precious metal deposition. *Econ. Geol.* **80**, 1640–1668.

Helgeson H. C. (1969) Thermodynamics of hydrothermal systems at elevated temperatures and pressures. *Am. J. Sci.* **267**, 729–804.

Henley R. W. and Ellis A. J. (1983) Geothermal systems, ancient and modern. *Earth Sci. Rev.* **19**, 1–50.

Ho P. C. and Palmer D. A. (1996) Ion association of dilute aqueous sodium hydroxide solutions to 600°C and 300 Mpa by conductance measurements. *J. Sol. Chem.* **25**, 711–729.

Johnson J. W., Oelkers E. H., and Helgeson H. C. (1992) SUPCRT92: A software package for calculating the standard molal thermodynamic properties of minerals, gases, aqueous species, and reactions from 1 to 5000 bars and 0 to 1000°C. *Comp. Geosci.* **18**, 899–947.

Lindsay W. T. Jr. (1980) Estimation of concentration quotients for ionic equilibria in high temperature water: The model substance approach. *Proc. Intl. Water Conf.* **41**, 284–294.

Mesmer R. E. and Baes C. F. Jr. (1974) Phosphoric acid dissociation equilibria in aqueous solutions to 300°C. *J. Soln. Chem.* **3**, 307–322.

Mountain B. W. and Wood S. A. (1988) Chemical controls on the solubility, transport, and deposition of platinum and palladium in hydrothermal solutions: A thermodynamic approach. *Econ. Geol.* **83**, 492–510.

Mountain B. W. and Seward T. M. (1999) The hydrosulphide/sulphide complexes of copper(I): Experimental determination of stoichiometry and stability at 22°C and reassessment of high temperature data. *Geochim. Cosmochim. Acta* **63**, 11–29.

Reed M. H. (1982) Calculation of multicomponent chemical equilibria and reaction processes in systems involving minerals, gases and an aqueous phase. *Geochim. Cosmochim. Acta* **46**, 513–528.

Seward T. M. (1981) The hydrothermal chemistry of gold and its implications for ore formation boiling and conductive cooling as examples. *Econ. Geol. Mon.* **6**, 398–404.

Seward T. M. and Barnes H. L. (1997) Metal transport by hydrothermal ore fluids. In *Geochemistry of Hydrothermal Ore Deposits*, 3rd ed. (ed. H. L. Barnes), pp. 435–486. Wiley-Interscience.

Suleimenov O. M. and Seward T. M. (1997) A spectrophotometric study of hydrogen sulphide ionisation in aqueous solutions to350°C. *Geochim. Cosmochim. Acta* **61**, 5187–5198.

Wood S. A. and Samson I. M. (1998) Solubility of ore minerals and complexation of ore metals in hydrothermal solutions. In *Techniques in Hydrothermal Ore Deposits* (J. Richards and P. Larson, eds.), pp. 33–80. Reviews in Economic Geology 10. Society of Economic Geologists.

Xiao Z., Gammons C. H., and Williams-Jones A. E. (1998) Experimental study of copper(I) chloride complexing at temperature from 40°C to 300°C and saturated vapor pressure. *Geochim. Cosmochim. Acta* **62**, 2949–2964.